




Thermal performance assessment of an energy lining for the Lyon-Turin base tunnel

Maria Romana Alvi¹ , Alessandra Insana¹ , Marco Barla^{1#} 

Article

Keywords

Energy tunnel
Thermal performance
Geothermal energy
Sensitivity analysis
Numerical coupled analysis

Abstract

The use of geothermal energy for heating and cooling purposes is an environmentally-friendly and cost-effective alternative with the potential to replace fossil fuels and help to mitigate global warming as well. The paper illustrates the geothermal potential evaluation of a portion of the Lyon-Turin base tunnel considering the thermal activation of the tunnel concrete segmental lining. The international infrastructure will connect Italy to France, crossing the Alps and meeting uncommon climate conditions, reaching a peak temperature of 47 °C, due to its significant rock overburden (up to 2500 m) under the Ambin massif. A thermo-hydraulic numerical model was used to simulate the heat exchange of the system and quantify the power achievable by thermally activating a 10 km-long section of the base tunnel. Sensitivity analyses were performed to investigate the influence of the heat carrier fluid and the air flow velocities as well as the inlet temperature on the heat exchange. Moreover, four different operational conditions were compared to allow for assessing the overall thermal performance of the energy lining in terms of heat exploited and of the capacity of cooling the tunnel.

1. Introduction

Despite the importance of the heating and cooling sector, renewable energy technologies currently supply only a small percentage of global and European heat demand per year (Seyboth et al., 2008; European Union, 2012; IEA, 2012) with the vast majority of heat currently generated by burning fossil fuels. However, sustainable solutions relying both on decreasing the consumption of non-renewable energy and developing technologies that harvest non-polluting energy sources are possible. The IPCC Special Report on Renewable Energy Sources and Climate Change Mitigation (IPCC, 2012) predicted the annual global CO₂ savings from renewable energy technologies in four deployment scenarios for 2030 and 2050 and highlighted the good potential of geothermal energy in reducing the greenhouse gas (GHG) emissions.

Geothermal energy is a good alternative to fossil fuels and its usage is among the most innovative and significant, contributing to environmental protection and providing substantial energy, long term cost savings and minimized maintenance (Kanth & Chakraborty, 2015).

So-called energy geostructures are earth-contact structures that embed a piping circuit with a circulating heat carrier fluid to achieve a heat exchange between the ground and any building or infrastructure (Brandl, 2006; Adam & Markiewicz, 2009; Barla & Perino, 2015). They combine the role of the structural support with the role of the thermal energy carrier in a unique technology to serve all types of buildings and infrastructure.

During recent years, increasing considerations have been paid on how this heat transfer technology could be extended to tunnels. In comparison with other energy geostructures, energy tunnels are characterized by their much more extensive linear development so that a bigger surface is in contact with the ground and can be thermally activated. Concerning the overburden and presence of potential heat end-users, considerable differences exist between city tunnels (metro lines, railway city crossings) and mountain tunnels (for railways and highways). Regarding the former, energy tunnels can serve as a renewable energy source for heating and cooling networks on a city scale (Epting et al., 2020; Baralis et al., 2020). In this context, a recent feasibility study was indeed carried out to assess the energy potential of the

[#]Corresponding author. E-mail address: marco.barla@polito.it

¹Politecnico di Torino, Department of Structural, Building and Geotechnical Engineering, Turin, Italy.

Submitted on January 18, 2022; Final Acceptance on February 4, 2022; Discussion open until May 31, 2022.

<https://doi.org/10.28927/SR.2022.000722>



This is an Open Access article distributed under the terms of the Creative Commons Attribution License, which permits unrestricted use, distribution, and reproduction in any medium, provided the original work is properly cited.

thermal activation of the Turin Metro line 2 (Barla et al., 2021). With reference to deep mountain tunnels, some insights on possible applications were given by Tinti et al. (2017) and Barla & Di Donna (2018) with reference to the Mules Access Tunnel of the Brenner Base Tunnel (BBT) and the Lyon-Turin tunnel. Additionally, Baralis et al. (2021) investigated the thermal activation of a tunnel lining in an Alpine context in relation to an application for bridge deck deicing showing that it can provide enough heat to keep the paved surface unfrozen.

In the case of TBM tunnelling, the absorber pipes can be tied to the reinforcement cage during the concrete segment prefabrication as for the 'Energietübbing' (Franzius & Pralle, 2011) and the 'Enertun' (Barla & Di Donna, 2016; Barla et al., 2019; Insana & Barla, 2020) systems. In the 'Enertun' system, two configurations exist, 'Ground' which comprehends a circuit of pipes installed nearby the extrados of the lining (surface in contact with the ground) and 'Air' where the pipes are closer to the intrados (surface in contact with the tunnel air).

This paper describes a possible application of the 'Air' configuration of the 'Enertun' system for a deep tunnel, namely the Lyon-Turin base tunnel, in a 10 km-long portion of the infrastructure under the huge cover of the Ambin massif. Thanks to the mining of the available geothermal energy potential due to the high rock mass and tunnel air

temperatures, not only a system able to exploit energy from a renewable resource (which would be otherwise ignored) could be achieved, but the tunnel internal climate conditions would be monitored and adjusted as well. In the following a description of the case study will be provided, followed by the presentation of numerical modelling setup and results.

2. The case study of the Lyon-Turin Base Tunnel

2.1 General description

The Lyon-Turin high-speed railway is a rail line under construction between the cities of Lyon (France) and Turin (Italy). It is intended to link the French and Italian high-speed rail networks and will be 270 km long. The core of the project is the Base Tunnel which will cross the Alps between the Susa Valley in Piedmont and the Maurienne in Savoie. The 57.5 km twin-tube tunnel beneath the Mont Cenis mountain, 45 km of which in France and 12.5 km on the Italian side, will replace the 150-year-old Frejus rail tunnel and will stand between 570 m and 750 m above sea level (Figure 1). Upon opening the tunnel, it will be the longest rail tunnel in the world, followed by the Gotthard

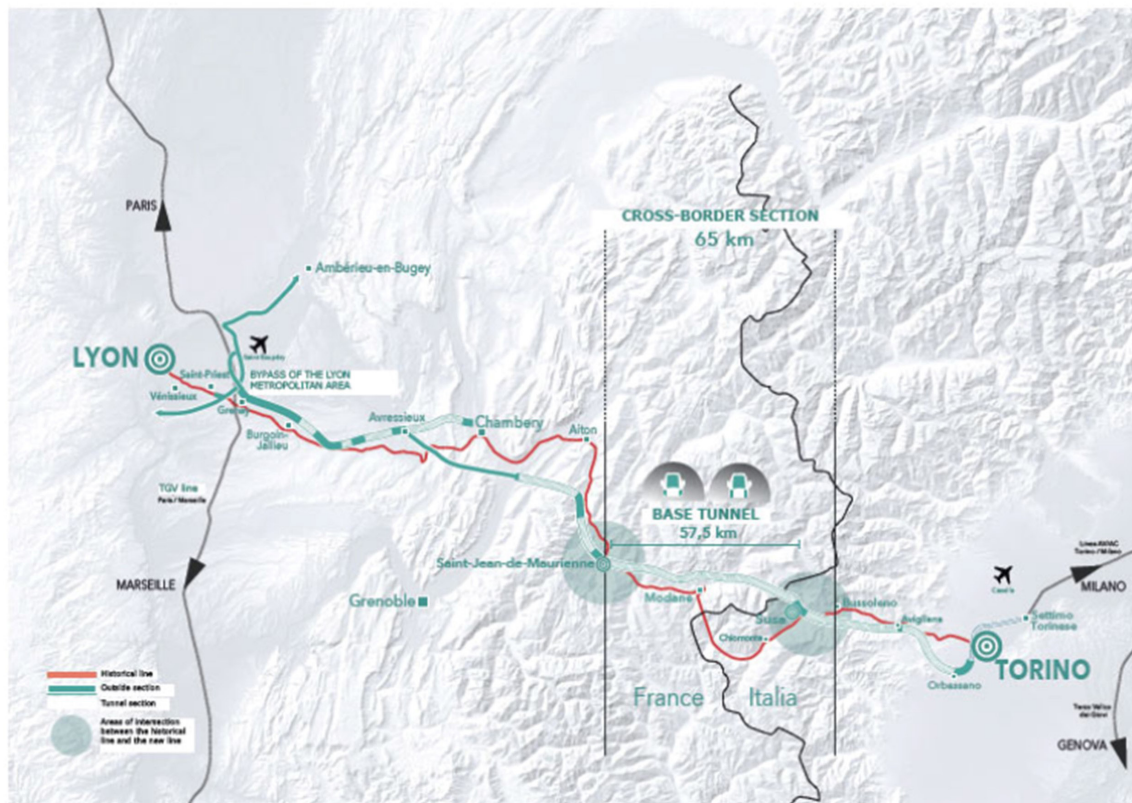


Figure 1. Cross-border section of the Lyon-Turin railway line overview (Italy, 2021).

Base Tunnel (57.1 km) and the Brenner Base Tunnel (55 km, currently under construction).

The reference geological and geomechanical model is based on the data obtained during the excavation of the inclined access adits at Saint-Martin-La-Porte, La Praz and Modane, including the La Maddalena exploratory tunnel (Bufalini et al., 2017). The base tunnel will encounter different geological contexts along its alignment including loose granular soils (alluvial deposits, glacial deposits), complex rock mass formations (arenaceous shale, coal-rich shale), evolutionary ground (anhydrites), high strength (mica schist and gneiss) or abrasive rock masses (quartzite). Thanks to the geological and geotechnical model developed, the most suitable methods to be adopted for excavation were identified, as well as the main geological risks, mitigation and management measures. Attention was devoted to critical conditions such as fault and severely fractured zones, high temperatures anomalies, squeezing, presence of swelling or soluble minerals. Hydrological investigations were carried out in order to assess the expected interference with aquifers such as water ingress into the tunnel and possible impacts on water resources, surface streams and rivers. Except for the first 350–400 m on the Susa side, the base tunnel is to be excavated with a slurry shield TBM (Tunnel Boring Machine), capable of creating a back pressure at the face greater than the groundwater hydrostatic pressure, in order to prevent water ingress into the tunnel. Immediately behind the TBM shield,

gaskets are to be adopted with the segmental lining to make it waterproof around the entire perimeter of the tunnel, when the water pressure is lower than 10 bar. Expected residual water flows at the portals are exploited for both drinking water and heating purposes (Bufalini et al., 2017).

2.2 The proposal for the thermal activation of a tunnel section

A specific study concerning the possible energy uses of the hot water intercepted during the excavation of the base tunnel in Chiomonte was recently carried out by TELT (2021). In this mentioned study, the heat exploited along the total length of the base tunnel (57.5 km), which ranges between 3.2 MW and 9.3 MW (for the least and the best conditions respectively), is to be used to supply a portion of the energy needs (district heating, swimming pools, greenhouses, etc.) of the Susa Valley. The close cities of Susa and Chiomonte for example could take advantage of this power to supply a swimming pool, greenhouses and the tunnel construction site area energy needs and for district heating.

From the geothermal profile evaluated for the base tunnel (Figure 2) it can be seen that in the core of the Ambin massif the temperature field reaches 47 °C, due to the overburden of 2500 m. This leads to the possibility of exploiting geothermal energy not only through the drained water but also by taking

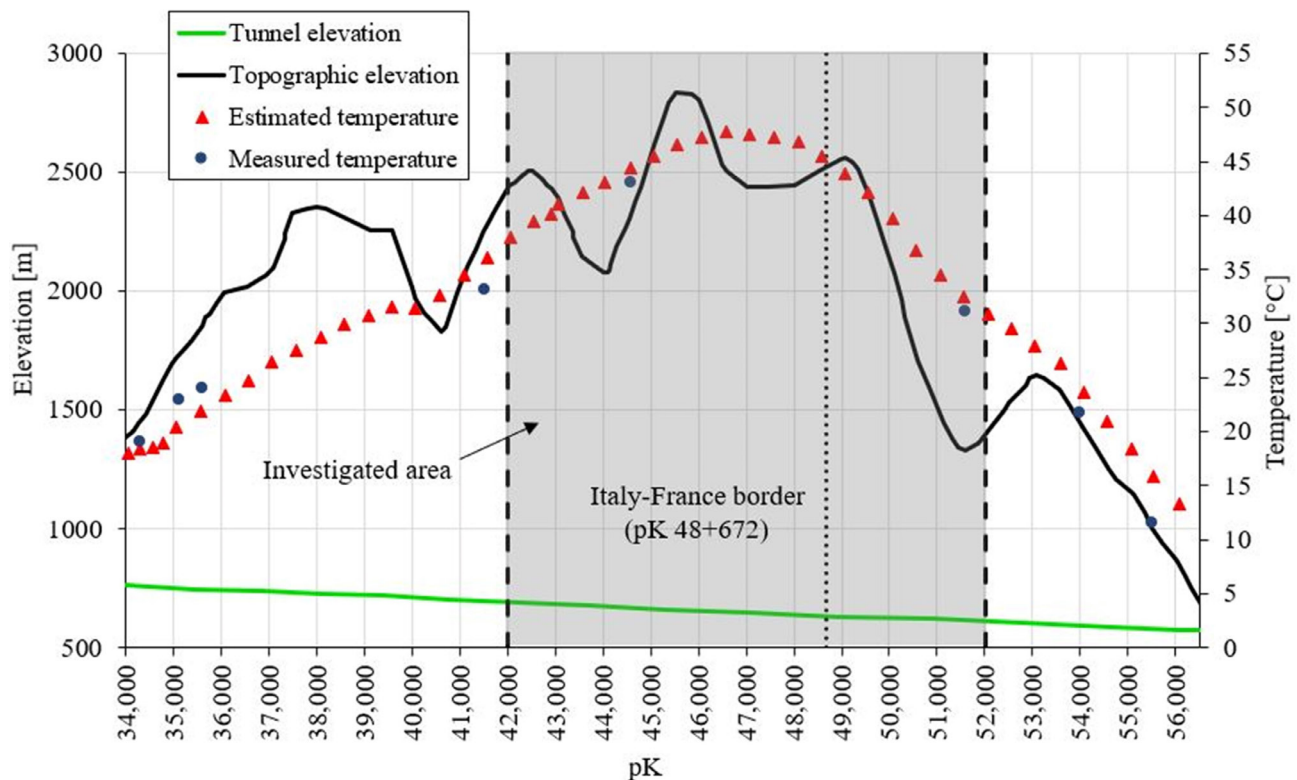


Figure 2. Geothermal profile of the Lyon-Turin railway base tunnel with indication of the investigated area (modified from LTF, 2001).

advantage of the high temperatures of the rock mass and of the air inside the infrastructure.

Diversely from prior studies, this paper will investigate the potential of thermally activating the tunnel lining thanks to the ‘Enertun’ system. The focus will be on the central 10 km-long section of the infrastructure (from pk 42 to pk 52, as shown in Figure 2) which also corresponds to the portion with the highest expected temperatures. The Air configuration of the ‘Enertun’ system is considered so that the circuit of embedded pipes is found at the intrados of the concrete lining segments and allows for heat exchange with the air inside the tunnel (Figure 3). The rings are hydraulically connected in pairs forming a subcircuit and the circuit of each segment is linked to that of the adjacent ones by hydraulic connections to form lining ring circuits (Barla et al., 2019; Rosso et al., 2021). The pipes are included in the concrete segments close to the internal boundary (at 10 cm from the air-lining interface), with a spacing of 30 cm, external diameter of 20 mm and thickness of 2.0 mm (cross-section area of 201 mm²).

The system may allow cooling the tunnel from the actual temperature down to the required working temperature (set to a maximal value of 32 °C by LTF, 2013). Potentially, the heat exploited during cooling of the 10 km-plant could be transferred to the nearest tunnel portal and used to satisfy energy needs in the area.

3. Description of the finite element model

To evaluate the potential of the proposed system described in 2.2, a 3D finite element model with thermo-hydraulic coupling was adopted. The thermo-hydraulic (TH) analyses were conducted by the software FEFLOW© (Diersch, 2009), where the thermo-hydraulic problem is governed by the following equations: the mass conservation, the Darcy’s law and the energy conservation for a saturated medium composed of a solid and a liquid (water) phase. In this chapter, the model set-up will be described together with the boundary conditions adopted and the thermo-physical properties of each component (surrounding ground, internal air and concrete energy lining).

The 3D model was built to reproduce a portion of the Lyon-Turin base tunnel, whose geometry is shown in Figure 4 with the indication of dimensions, materials and boundary conditions. It is composed of 240537 nodes and 465048 triangular prismatic three-noded elements distributed in 37 slices. A 30 cm-thick segmental lining with an outer diameter of 9 m was adopted. The whole domain is 200 m high and 200 m wide so that both the height and width are equal to twenty times the outer tunnel diameter, which allows the boundary effects to be ignored. The modelled tunnel has a longitudinal length of 8.4 m with 6 rings of a hypothesizing length of 1.4 m, each ring composed of 6 concrete segments. The absorber pipes were reproduced by 1D elements called

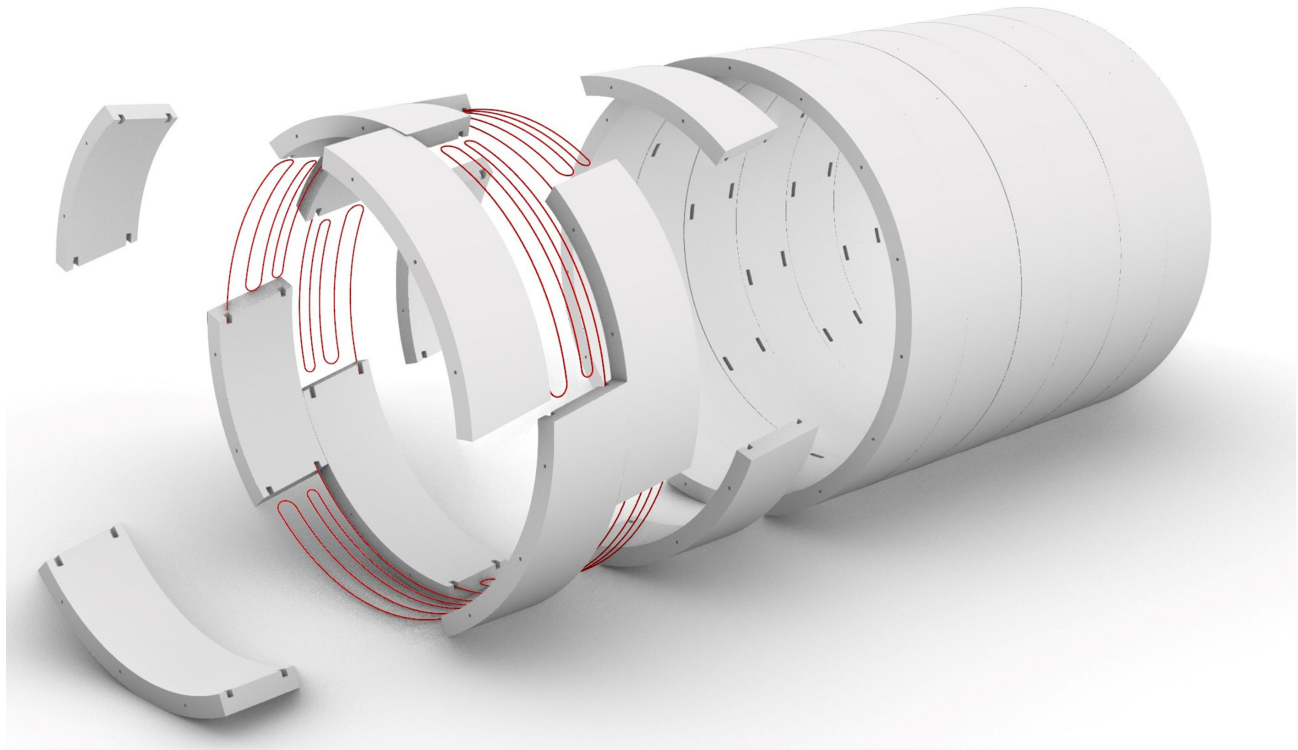


Figure 3. Exploded view of the ‘Air’ pipes embedded in the segmental lining.

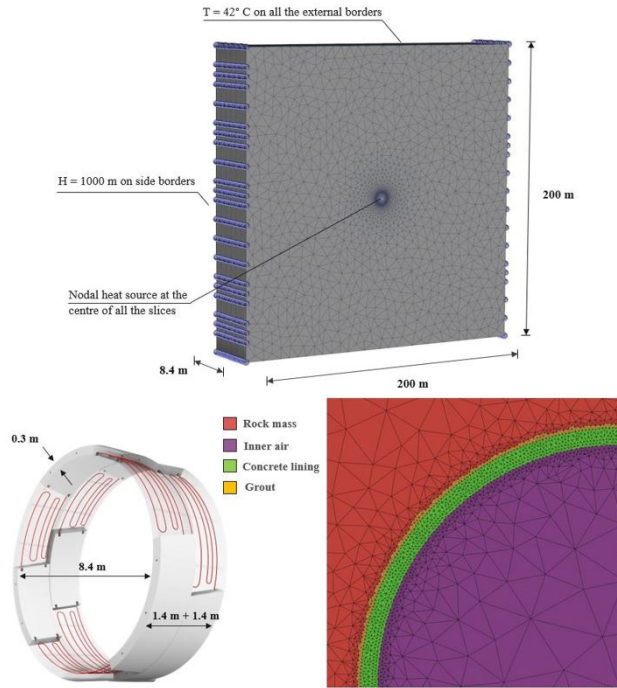


Figure 4. 3D FEM model with the indication of external and internal dimensions, materials and boundary conditions.

“discrete features” (distributed throughout the tunnel as shown in Figure 5), provided by the software FEFLOW®. Their properties are summarized in Table 1.

In these elements, the thermal resistance of the plastic pipes is neglected. This could lead to a very small temperature error in terms of numerical analysis results. However, the use of the 1D pipe elements was validated for similar systems and showed good agreement when compared to analytical solutions (Diersch, 2009). The mass and energy conservation equations governing the convection-diffusion problem, are satisfied for these elements, while the fluid flow inside them is described by the Hagen–Poiseuille law. Accordingly, fluid particles are assumed to move in pure translation with constant velocity, similarly to what occurs in circular tubes. An insulation layer able to prevent heat losses was placed around the network of pipes along the connection from the first to the second ring (and from the third to the fourth and so on) like it would be in reality, although in the model the connection takes place within the rock mass. The internal air was also discretized not only to investigate the heat exchange between the absorber pipes and the tunnel environment but also to monitor the internal climate conditions. The material properties were assigned to all the elements of the model, adding a 10 cm-thick layer of grout between the concrete lining and the surrounding ground for the sake of likelihood (Figure 4). All the thermo-hydraulic material properties are listed in Table 2.

Considering the scale of the problem, an equivalent continuum model was considered appropriate to represent

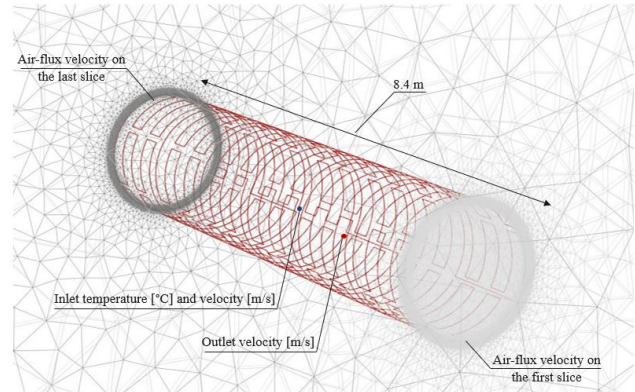


Figure 5. 3D discretisation of the piping system in the lining segments and boundary conditions.

Table 1. Discrete features properties adopted for the simulation of absorber pipes.

Property	Symbol	Unit	Value
External diameter	D	mm	20
Tube thickness	s	mm	2
Spacing	i	mm	300
Cross-sectional area	A	mm ²	201.06
Hydraulic aperture	r_{yd}	mm	8.0

the surrounding fractured rock mass. Due to the presence of discontinuities, the thermal conductivity of the rock mass is expected to be lower than that of the intact rock. This effective conductivity parameter depends on multiple factors such as fracture density, trace length and fracture thermal contact resistance (Li et al., 2021). Because of the preliminary stage of the analysis, such information could not be retrieved for the fracture network present in the studied area and the intact rock value was assumed for the following analyses. This may lead to computing a higher outlet temperature of the heat carrier inside the pipes and, thus, a slightly higher exploitable thermal power. Despite the Authors believe that this will only marginally affect the results obtained, it is an aspect that should be more deeply explored in a future stage of the research.

The fractures in the rock mass are supposed to be completely saturated and no flow occurs. To consider this, a constant hydraulic head of 1000 m was set all over the domain as an initial condition and at the lateral sides of the model. Moreover, a temperature of 42 °C (mean value of the estimated temperatures at the tunnel depth, Figure 2) was set throughout the domain as the initial condition and fixed equal at all the edges of the model. A heat nodal boundary condition of -12 W was imposed in the central node of the tunnel cross-section, reproducing a constant injection of thermal energy to simulate the possible increase of the internal air temperature due to fast-moving vehicles or additional sources of heat (shown in Figure 4).

Table 2. Thermo-hydraulic material properties.

Material	Property	Symbol	Unit	Value
Ground	Horizontal hydraulic conductivity	$K_x = K_z$	m/s	$4.1 \cdot 10^{-8}$
	Vertical hydraulic conductivity	K_y	m/s	$4.1 \cdot 10^{-8}$
	Specific storage	S	m^{-1}	10^{-4}
	Porosity	n	—	0.02
	Fluid-phase thermal conductivity	λ_w	W/ (m ¹ K ¹)	0.65
	Solid-phase thermal conductivity	λ_s	W/ (m ¹ K ¹)	2.74
	Fluid-phase volumetric thermal capacity	$\rho_w c_w$	MJ/ (m ³ K ¹)	4.2
	Solid-phase volumetric thermal capacity	$\rho_s c_s$	MJ/ (m ³ K ¹)	2.4
	Transverse aquifer thermal dispersivity	α_T	m	0.5
	Longitudinal aquifer thermal dispersivity	α_L	m	5
Tunnel lining	Specific storage	S	m^{-1}	10^{-4}
	Solid-phase thermal conductivity	λ_s	W/ (m ¹ K ¹)	1.5
	Solid-phase volumetric thermal capacity	$\rho_s c_s$	MJ/ (m ³ K ¹)	2.19
	Horizontal hydraulic conductivity	$K_x = K_z$	m/s	10^{-16}
	Vertical hydraulic conductivity	K_y	m/s	10^{-16}
	Porosity	n	—	0
Grout	Specific storage	S	m^{-1}	10^{-4}
	Solid-phase thermal conductivity	λ_s	W/ (m ¹ K ¹)	2.0
	Solid-phase volumetric thermal capacity	$\rho_s c_s$	MJ/ (m ³ K ¹)	2.19
	Horizontal hydraulic conductivity	$K_x = K_z$	m/s	10^{-16}
	Vertical hydraulic conductivity	K_y	m/s	10^{-16}
	Porosity	n	—	0
Insulation	Specific storage	S	m^{-1}	10^{-4}
	Solid-phase thermal conductivity	λ_s	W/ (m ¹ K ¹)	0.0255
	Solid-phase volumetric thermal capacity	$\rho_s c_s$	MJ/ (m ³ K ¹)	0.001
	Horizontal hydraulic conductivity	$K_x = K_z$	m/s	10^{-16}
	Vertical hydraulic conductivity	K_y	m/s	10^{-16}
	Porosity	n	—	0
Internal air	Specific storage	S	m^{-1}	10^{-4}
	Fluid-phase thermal conductivity	λ_w	W/ (m ¹ K ¹)	0.53
	Fluid-phase volumetric thermal capacity	$\rho_w c_w$	MJ/ (m ³ K ¹)	10^{-3}
	Horizontal hydraulic conductivity	$K_x = K_z$	m/s	10^{-2}
	Vertical hydraulic conductivity	K_y	m/s	10^{-2}
	Porosity	n	—	1
	Transverse thermal dispersivity	α_T	m	0.5
	Longitudinal thermal dispersivity	α_L	m	5

To simulate the environment inside the tunnel and the geothermal plant operation conditions, a proper air-flux velocity at the first and last model slices and an inlet fluid temperature and velocity, regarding the absorber pipes, at the beginning of the circuit must be added. Also, an outlet fluid velocity has to be set at the end of the pipes network. These additional boundary conditions applied are shown in Figure 5. Given the influence involving these last parameters, it was chosen to perform sensitivity analyses, whose results will be discussed in the next chapter (section 4.1).

4. Numerical modelling results

In this chapter, the results of the thermo-hydraulic (TH) coupled analyses performed will be described. A first

section will focus on some sensitivity analyses to assess the proper boundary value parameters with respect to the air-flux velocity, the temperature and the velocity of the heat carrier fluid. Then the attention is posed on the short and long term behaviour of the thermoactive system so to quantify the amount of exploitable geothermal energy in different operating modes.

To investigate the thermal feasibility of energy geostructures, when the pipes are explicitly modelled, the exchanged heat can be computed from the results of the numerical analysis, as in Equation 1:

$$Q = mc(T_{in} - T_{out}) \quad (1)$$

where Q (in Watt) is the exploitable heat of the site, m (in kg/s) is the mass flow rate, c (in $J \cdot kg^{-1} \cdot ^\circ C^{-1}$) is the heat capacity of the circulating fluid at constant pressure, T_{in} (in $^\circ C$) is the inlet temperature and T_{out} (in $^\circ C$) is the outlet temperature of the heat carrier fluid running in the pipes.

4.1 Sensitivity analyses

The tunnel internal air is influenced by the motion of the vehicles running into it and, especially for railways and motorways tunnels, this needs to be accounted for when analysing the thermal behaviour of the infrastructure. Thus, a parametric analysis on the air-flux velocity was performed, showing that a higher flow velocity is able to facilitate the heat distribution inside the tunnel, while with a lower air-flux a more inhomogeneous distribution of the air temperature was seen both radially and axially. Based on this, a constant value of 8 m/s was imposed on the air nodes of the first and last cross-section of the numerical model in the subsequent analyses. The adoption of this value represents the most conservative choice among all the investigated velocities since the temperatures at the intrados of the lining were the highest experienced amongst all.

A second set of parametric analyses were conducted to study the influence of the inlet velocity and temperature of the heat carrier fluid. Such initial and boundary conditions have been varied one by one to determine the most suitable pair and optimise the plant performance. The operational conditions of the geothermal system were simulated by circulating fluid in the pipes network at a given inlet temperature and velocity, defined as Dirichlet and Neumann boundary conditions

respectively. Figure 6a shows the difference between the inlet and outlet fluid temperature (which influences the heat exchanged according to Equation 1) computed as a function of the heat carrier fluid velocity and temperature. Figure 6b depicts the thermal power calculated, in kW/m and after 1 year of continuous heat extraction, for a certain combination of fluid velocity and inlet temperature. It is evident that, for the tested ranges, the lower the temperature the higher the quantified exploitable heat, along with a higher fluid velocity. From the picture, it can also be seen that the fluid input temperature (ranging between 20–28 $^\circ C$) was the parameter that mostly affected the heat exchange in terms of exploitable geothermal power, at least from a certain heat carrier fluid velocity onwards.

Finally, the optimal input values were selected looking also at the difference ΔT between the outlet fluid temperature and that of the undisturbed rock mass at the end of the year investigated. A bigger difference would lead to a higher geothermal power per meter and a dimensionally less costly geothermal plant, but, at the same time, it would imply the worse performance of the heat pump, also affecting the ground thermal equilibrium. For this reason, to properly balance the heat pump efficiency with the overall system dimensions, a maximum of 17 $^\circ C$ was adopted as the limit value between the outlet fluid temperature and that of the undisturbed ground (Capozza et al., 2012). Based on the above, 24 $^\circ C$ and 0.8 m/s were imposed on the first node of the absorber pipes circuit, in the first, third and fifth ring, as this combination allowed to fulfil the above mentioned limit value and to maximise thermal power. From now onwards, the

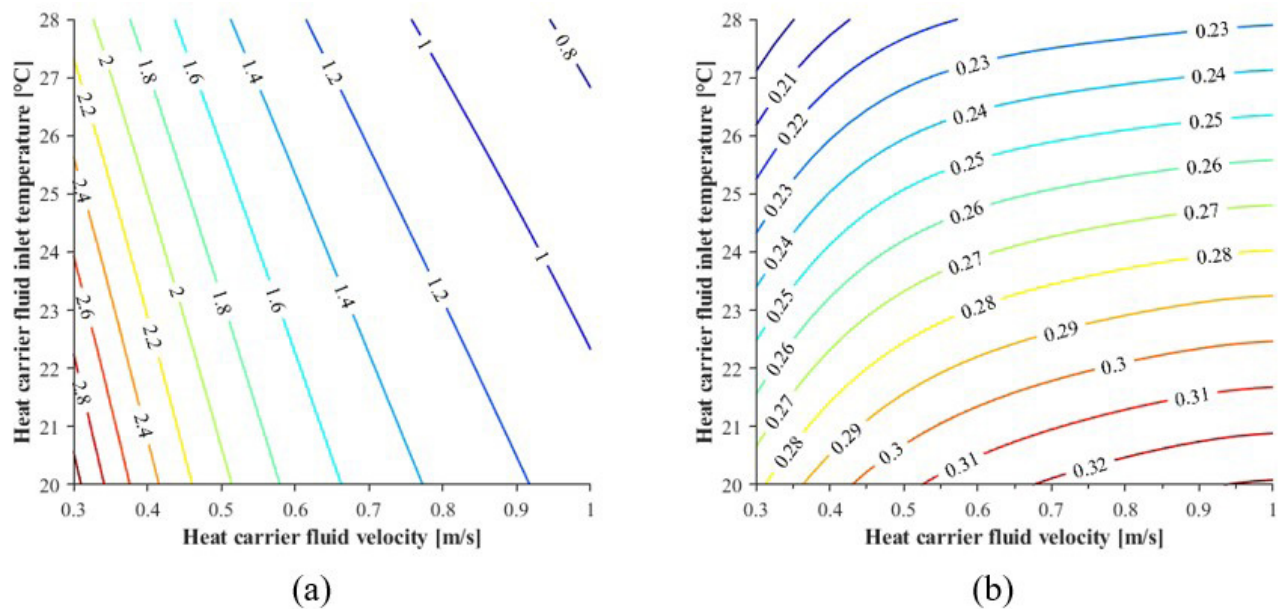


Figure 6. (a) Difference ($^\circ C$) between the outlet and inlet fluid temperature; and (b) thermal power (kW/m) exploited at the end of the year investigated depending on the fluid velocity and inlet temperature.

numerical simulations will refer only to the results obtained adopting these two boundary values for the heat carrier fluid.

4.2 Short term behaviour

The optimised model was used to quantify the heat that could be exchanged with the tunnel internal environment and the surrounding ground all over the year. Four types of operating conditions have been studied:

- the geothermal heat exchanger is active all the year-round,
- the geothermal heat exchanger is suspended during the summer season (three months),
- the geothermal heat exchanger is suspended for a longer period (five months from May to September),
- the geothermal heat exchanger is activated cyclically monthly (with on-and-off cycles for the heat pump being 30 days long).

To apply the above conditions, the temperature and velocity boundary conditions were imposed to the corresponding nodes through time histories in which the fluid motion circulation in the pipes is controlled. The imposed inlet temperature and the computed outlet temperature during the first year of the TH numerical simulations are shown in Figure 7 for each operational mode. The beginning of the analysis ($t=0$) corresponds to January, while the summer period (considering it from June to September) goes from day 151 to 243.

The computed temperature difference, the power per meter and the total power for the 10 km long section (considering that the inlet fluid temperature corresponds to 24 °C after 365 days of service) are shown in Table 3. Except for the continuous operating condition a), at the end of the first year, the geothermal plant would be able to extract at least 3 MW of thermal power for the base tunnel length

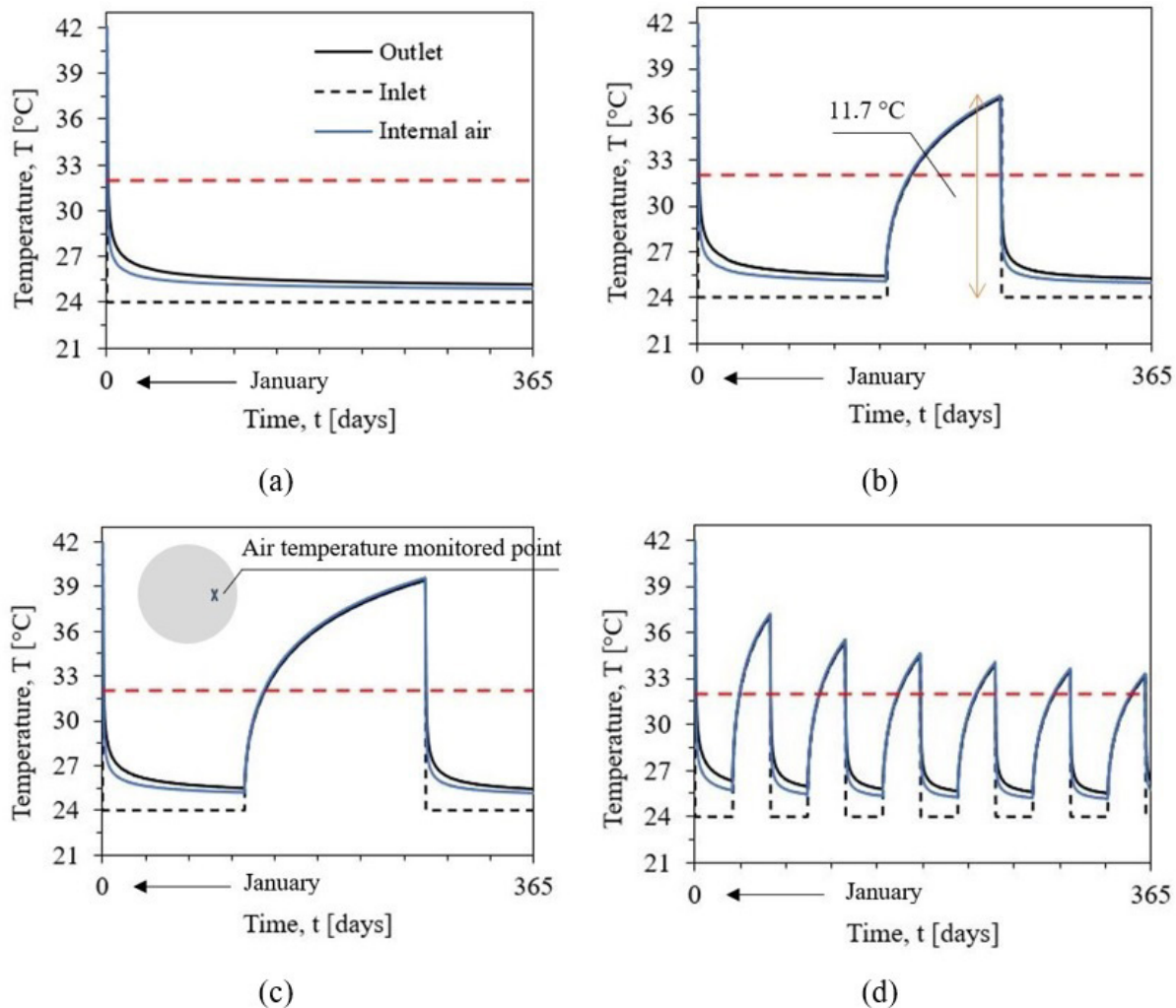


Figure 7. Imposed inlet temperature, computed outlet temperature and internal air temperature for (a) continuous; (b) cyclic (no 3 months); (c) cyclic (no 5 months); and (d) cyclic monthly activation (in red is the established temperature threshold of 32 °C for internal air).

Table 3. Temperature difference (ΔT), thermal power per meter of tunnel (q) and total power for the 10 km section (Q) in all the operating conditions considered.

Operating mode	Time	ΔT (°C)	q (kW/m)	Q (MW)
a) Continuous	1 year	1.14	0.28	2.84
	10 years	0.75	0.18	1.81
b) Cyclic (no 3 months)	1 year	1.27	0.30	3.04
	10 years	0.88	0.21	2.11
c) Cyclic (no 5 months)	1 year	1.46	0.34	3.43
	10 years	1.04	0.25	2.51
d) Cyclic monthly activation	1 year	1.50	0.36	3.61
	10 years	1.06	0.26	2.55

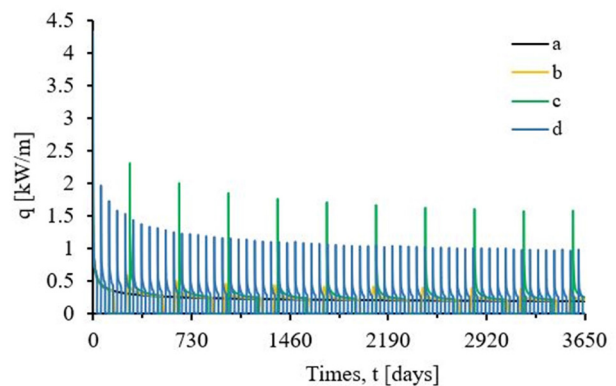
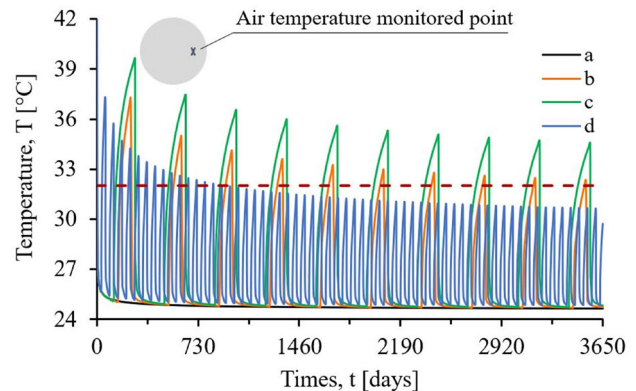
examined, with a maximum of 3.6 MW if the heat pump worked according to mode d).

The importance of seasonal activation is the need to avoid source depletion. The constant heat extraction of the continuous mode a), in fact, and the absence of groundwater flow will decrease the efficiency of the heat pump in the long term (Capozza et al., 2012). To avoid this, temporary breaks are introduced with the operating modes b), c) and d) to facilitate the thermal recharge of the ground. This would also result in a temperature variation of the tunnel internal environment. For example, in the operating mode b), during the three months in which the geothermal plant is switched off the climate conditions inside the tunnel would rise of about 11.7 °C (Figure 7b). Surely, in the first year at least, the continuous operating mode is the only one of those considered able to keep the internal air temperature under the acceptable limit of 32 °C (Figure 7a) imposed by LTF (2013). For such reason, there would be no need for a ventilation system implementation.

4.3 Exploitation in the long-term

To study the performance of the geothermal system in the long term, the coupled thermo-hydraulic analyses considering the four operational modes described above have been extended to a 10-year timespan. The results obtained in terms of specific thermal power are presented in Figure 8. As years go by, thermal efficiency changes in a different way depending on the operational mode considered, as quantified in Table 3.

In the long term, the system would provide a geothermal power per meter ranging between 0.18 and 0.26 kW/m, looking at all the scenarios. In terms of comparison, the power per meter evaluated by TELT (2021) with the exploitation of the drainage water heat would amount to around 0.162 kW/m in its most advantageous condition. According to the preliminary estimations shown, the thermal power per meter obtained through the thermal activation of the lining is similar, and even more favourable in selected cases. An additional advantage of the studied technology is that the system is a closed-loop

**Figure 8.** Extracted power per meter of tunnel with (a) continuous; (b) cyclic (no 3 months); (c) cyclic (no 5 months); and (d) cyclic monthly activation.**Figure 9.** Internal air temperature with (a) continuous; (b) cyclic (no 3 months); (c) cyclic (no 5 months); and (d) cyclic monthly activation (in red is the established temperature threshold of 32 °C for internal air).

and allows to avoid direct influence on the groundwater, reducing the concurrent environmental problems.

Lastly, Figure 9 presents the monitored internal air temperature. In comparison to the conditions experienced in

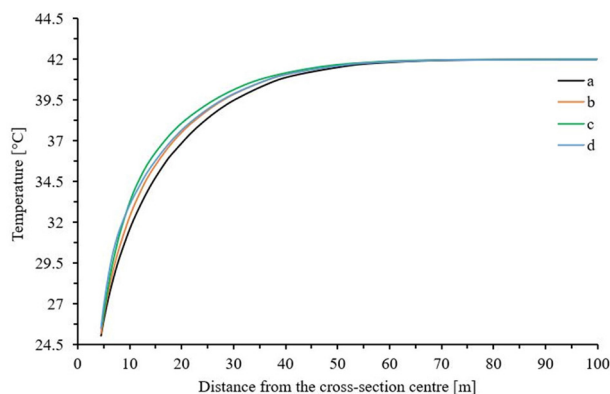


Figure 10. Worst scenario of ground temperature versus distance from the tunnel contour for (a) continuous; (b) cyclic (no 3 months); (c) cyclic (no 5 months); and (d) cyclic monthly activation.

the short-term (section 4.2) and with respect to the seasonal working modes b) and c), the 10 year-long analyses show a less pronounced growth of the internal air temperatures during the periods in which the geothermal plant is switched off. Specifically in the last year of the numerical analysis performed adopting mode b), the internal temperature during the three summer months of suspension will rise of just 7.3 °C, against the 11.7 °C of the first year (Figure 7b). However, the maximum limit of 32 °C imposed by LTF (2013) was only slightly exceeded for this case. On the contrary, assuming the cyclic monthly activation (mode d) for the heat pump, the tunnel internal air temperature, after 2 years and a half from the beginning of the heat extraction, would be maintained under this maximum value, as experienced with the continuous scenario a) (Figure 9).

Finally, the influence of the thermal activation on the surrounding ground temperature was checked for all the operating modes. Figure 10 depicts the temperature profile from the tunnel lining extrados to the model external boundary for modes a), b), c) and d) in their worst scenario, i.e. when the highest temperature reduction is experienced. For the operating mode a) and d), this corresponds to the end of the tenth year. Whereas, for mode b) and c), this condition occurs just before the seasonal break of the tenth year. In all situations, the ground affected zone lies within 50 m from the tunnel contour. However this trend is more or less constant only for mode a) while, for the other modes, it experiences variations throughout the year depending on the actual state of operation of the system (on/off cycles).

5. Conclusions

This work presents a numerical study conducted to evaluate the performance of the thermal activation of the tunnel linings for a 10 km-long section of the Lyon-Turin base tunnel. The aim is to take advantage of the high temperatures

expected at the base tunnel depth, exploit geothermal energy and, at the same time, improve the tunnel internal climate conditions. The portion of the base tunnel investigated fits into the category of hot tunnels, mainly due to the overburden, exceeding 2 km, experienced in the core of the Ambin massif. In addition, fast-moving trains or vehicles also contribute to raising the internal air temperature above the acceptable limits, and, hence, cooling is needed.

To enhance the heat exchange with the internal environment, the ‘Enertun air’ configuration of the circuit embedded into the concrete segmental lining was supposed to be installed.

Sensitivity analyses allowed to assess the most suitable boundary conditions for the inlet temperature and velocity of the fluid running into the absorber pipes. The ultimate values adopted in the model were an inlet temperature of 24 °C and a fluid velocity of 0.8 m/s, considering the exchangeable heat and the difference between the outlet fluid temperature and that of the undisturbed ground. The proper air-flux has been investigated as well and a velocity of 8 m/s has been set.

Four different theoretical scenarios for the geothermal plant behaviour have been considered to calculate the heat exchange obtained in the context investigated. The main issue was to find a satisfying compromise between the simulated most profitable thermal activation, in terms of exploitable power, and a safe internal climate (as assigned by LTF, 2013). With a continuous operating mode a), after 10 years the thermal power per meter is around 0.18 kW/m and the internal air temperature is maintained under the maximum limit (32 °C). In the other three hypotheses (b, c and d), cyclic operating conditions were implemented. Two of them (b and c) were seasonal, with the suspension of the heat extraction for three or five months, able to provide respectively 0.21 and 0.25 kW/m in a 10-year lifespan. In the last case d), the overall system was supposed to be activated according to monthly on-off cycles providing almost 0.26 kW/m in the long term. Acceptable climate conditions inside the tunnel were obtained for mode b) and d) after 10 and 2.5 years respectively, while it was not obtained in the 10 years period for operating mode c).

In conclusion, the ideal operating mode depends on the specific aim of the thermal activation project envisaged. If a constant energy provision along the year is requested, the continuous mode a) is to be chosen, also gaining in terms of cooling of the tunnel with relevant savings on ventilation and cooling system costs. In particular, if the focus is posed on the ventilation aspect, a cyclic monthly activation (mode d) should be evaluated as well, which develops a profitable geothermal plant in terms of power per meter, albeit it works for just half a year. Also mode b) may provide a reasonable compromise. In case the deep tunnel cooling is not mandatory, the seasonal alternative c) is another viable solution as it produces relevant thermal power. Nevertheless, the four operating modes represent theoretical limit conditions. In case of real operation, an equilibrium with the thermal needs should be sought thus implying on-and-off cycles designed ad hoc.

The work performed testifies that the ‘Enertun Air’ energy lining can be a highly competitive alternative, as a closed-loop system, to the thermal use of drainage water, also thanks to its additional advantages in terms of minor disturbance to the groundwater and the possibility to regulate the tunnel inner climate with savings on ventilation and cooling costs.

Declaration of interest

The authors have no conflicts of interest to declare. All co-authors have observed and affirmed the contents of the paper and there is no financial interest to report.

Authors’ contributions

Maria Romana Alvi: conceptualization, Data curation, Formal Analysis, Investigation, Methodology, Validation, Visualization, Writing – original draft, Writing – review & editing. Alessandra Insana: conceptualization, Data curation, Formal Analysis, Investigation, Methodology, Supervision, Visualization, Writing – review & editing. Marco Barla: conceptualization, Funding acquisition, Investigation, Methodology, Project administration, Resources, Supervision, Visualization, Writing – review & editing.

List of symbols

A	cross-sectional area of pipes
D	diameter
c	heat capacity of the circulating fluid at constant pressure
c_s	heat capacity of the solid phase
c_w	heat capacity of the liquid phase
H	hydraulic head
i	spacing
K_x, K_z, K_y	horizontal and vertical hydraulic conductivity
m	mass flow rate
n	porosity
q	thermal power per meter
Q	exchangeable heat in Watt
r_{yd}	hydraulic aperture
s	thickness
S	specific storage
T	temperature
T_{in}	Inlet temperature of the heat carrier fluid
T_{out}	Outlet temperature of the heat carrier fluid
v	velocity
α_L	longitudinal thermal dispersivity
α_T	transverse thermal dispersivity
λ_s	solid phase thermal conductivity
λ_w	liquid phase thermal conductivity
ρ_s	solid phase density
ρ_w	water or liquid phase density

References

- Adam, D., & Markiewicz, R. (2009). Energy from earth-coupled structures, foundations, tunnels and sewers. *Geotechnique*, 59(3), 229-236. <http://dx.doi.org/10.1680/geot.2009.59.3.229>.
- Baralis, M., Barla, M., Bogusz, W., Di Donna, A., Ryżyński, G., & Żeruć, M. (2020). Geothermal potential of the NE extension Warsaw (Poland) metro tunnels. *Environmental Geotechnics*, 7(4), 282-294. <http://dx.doi.org/10.1680/jenge.18.00042>.
- Baralis, M., Insana, A., & Barla, M. (2021). Energy tunnel for deicing of a bridge deck in Alpine region. In *International Conference of the International Association for Computer Methods and Advances in Geomechanics. Challenges and Innovations in Geomechanics (IACMAG 2021)* (Lecture Notes in Civil Engineering, No. 126, pp.1061-1068). Cambridge: Springer. http://dx.doi.org/10.1007/978-3-030-64518-2_126.
- Barla, M., & Di Donna, A. (2016). Conci energetici per il rivestimento delle gallerie. *Strade & Autostrade*, 5(119), 46-49.
- Barla, M., & Di Donna, A. (2018). Energy tunnels: concept and design aspects. *Underground Space*, 3(4), 268-276. <http://dx.doi.org/10.1016/j.undsp.2018.03.003>.
- Barla, M., & Perino, A. (2015). Energy from geo-structures: a topic of growing interest. *Environmental Geotechnics*, 2(1), 3-7. <http://dx.doi.org/10.1680/envgeo.13.00106>.
- Barla, M., Baralis, M., Insana, A., Santina, A., Antolini, F., Vigna, F., Azzarone, F., & Marchetti, P. (2021). On the thermal activation of Turin Metro Line 2 Tunnels. In *International Conference of the International Association for Computer Methods and Advances in Geomechanics. Challenges and Innovations in Geomechanics. IACMAG 2021* (Lecture Notes in Civil Engineering, No. 126, pp. 1069-1076). Cambridge: Springer. https://doi.org/10.1007/978-3-030-64518-2_127.
- Barla, M., Di Donna, A., & Insana, A. (2019). A novel real-scale experimental prototype of energy tunnel. *Tunnelling and Underground Space Technology*, 87, 1-14. <http://dx.doi.org/10.1016/j.tust.2019.01.024>.
- Brandl, H. (2006). Energy foundations and other thermo-active ground structures. *Geotechnique*, 56(2), 81-122. <http://dx.doi.org/10.1680/geot.2006.56.2.81>.
- Bufalini, M., Dati, G., Rocca, M., & Scevaroli, R. (2017). The Mont Cenis Base Tunnel. *Geomechanics and Tunnelling*, 10(3), 246-255. <http://dx.doi.org/10.1002/geot.201700009>.
- Capozza, A., De Carli, M., Galgaro, A., & Zarrelle, A. (2012). *Linee guida per la progettazione dei campi geotermici per pompe di calore*. Milan: RSE (in Italian).
- Diersch, H.J.G. (2009). *DHI wasy software – Feflow 6.1 – Finite element subsurface flow & transport simulation system: reference manual*. Berlin: DHI-WASY GmbH.
- Epting, J., Baralis, M., Künze, R., Mueller, M. H., Insana, A., Barla, M., & Huggenberger, P. (2020). Geothermal potential

- of tunnel infrastructures: development of tools at the city-scale of Basel, Switzerland. *Geothermics*, 83, 101734. <http://dx.doi.org/10.1016/j.geothermics.2019.101734>.
- European Union. (2012). *EU - Energy in figures: statistical pocketbook 2012*. Luxembourg: European Commission. Retrieved in August 15, 2013, from <https://data.europa.eu/doi/10.2833/11169>
- Franzius, J.N., & Pralle, N. (2011). Turning segmental tunnels into sources of renewable energy. *Proceedings of the Institution of Civil Engineers. Civil Engineering*, 164(1), 35-40. <http://dx.doi.org/10.1680/cien.2011.164.1.35>.
- Insana, A., & Barla, M. (2020). Experimental and numerical investigations on the energy performance of a thermo-active tunnel. *Renewable Energy*, 152, 781-792. <http://dx.doi.org/10.1016/j.renene.2020.01.086>.
- Intergovernmental Panel on Climate Change – IPCC. (2012). *Renewable energy sources and climate change mitigation: summary for policymakers and technical summary*. Cambridge: Cambridge University Press.
- International Energy Agency – IEA. (2012). *Policies for renewable heat: an integrated approach* (Insight Series 2012). Paris: OECD/IEA.
- Italy. Ministero delle Infrastrutture e della Mobilità Sostenibili - MIMS. (2021). *Torino-Lione: al Piemonte 32 milioni di euro per opere di tutela ambientale e sociale*. Rome. Retrieved in August 15, 2013, from <https://mit.gov.it/> (in Italian).
- Kanth, A., & Chakraborty, T. (2015). Numerical analysis of geothermal tunnels. *IJRET: International Journal of Research in Engineering and Technology*, 4(2), 740-746. <http://dx.doi.org/10.15623/ijret.2015.0402102>.
- Li, Z.W., Liu, Y., Mei, S.M., Xing, S.C., & Wang, X.K. (2021). Effective thermal conductivity estimation of fractured rock masses. *Rock Mechanics and Rock Engineering*, 54(12), 6191-6206. <http://dx.doi.org/10.1007/s00603-021-02599-5>.
- Lyon Turin Ferroviarie – LTF. (2001). *Nuova linea Torino Lione: progetto preliminare in variante. Complementi di geologia – Modello geotermico*. Chambéry, France (in Italian).
- Lyon Turin Ferroviarie – LTF. (2013). *Ventilazione: studio degli scenari di estrazione fumi dal tunnel (Revisione del progetto definitivo)*. Chambéry, France (in Italian).
- Rosso, E., Insana, A., Vesipa, R., & Barla, M. (2021). Optimization of the hydraulic circuit for energy tunnels. In *EURO:TUN 2021, 5th International Conference on Computational Methods and Information Models in Tunneling*. Bochum: Ruhr University Bochum.
- Seyboth, K., Beurskens, L., Langniss, O., & Sims, R.E. (2008). Recognizing the potential for renewable energy heating and cooling. *Energy Policy*, 36(7), 2460-2463. <http://dx.doi.org/10.1016/j.enpol.2008.02.046>.
- Tinti, F., Boldini, D., Ferrari, M., Lanconelli, M., Kasmaee, S., Bruno, R., Egger, H., Voza, A., & Zurlo, R. (2017). Exploitation of geothermal energy using tunnel lining technology in a mountain environment: a feasibility study for the Brenner Base tunnel – BBT. *Tunnelling and Underground Space Technology*, 70, 182-203. <http://dx.doi.org/10.1016/j.tust.2017.07.011>.
- Tunnel Euralpin Lyon-Turin – TELT. (2021). *Acqua: Energia dal tunnel di base. La risorsa geotermica come opportunità di sviluppo green. TELT e dipartimenti DIATI e DENERG del Politecnico di Torino*. Italy (in Italian).